

When AI Levels the Playing Field: Skill Homogenization, Asset Concentration, and Two Regimes of Inequality

Xupeng Chen* Shuchen Meng[†]

March 10, 2026

Abstract

Generative AI compresses within-task skill differences while shifting economic value toward concentrated complementary assets, creating an apparent paradox: the technology that equalizes individual performance may widen aggregate inequality. We formalize this tension in a task-based model with endogenous education, employer screening, and heterogeneous firms. The model yields two regimes whose boundary depends on AI’s technology structure (proprietary vs. commodity) and labor market institutions (rent-sharing elasticity, asset concentration). A scenario analysis via Method of Simulated Moments, matching six empirical targets, disciplines the model’s quantitative magnitudes; a sensitivity decomposition reveals that the five non- Δ Gini moments identify mechanism rates but not the aggregate sign, which at the calibrated parameters is pinned by m_6 and ξ , while AI’s technology structure (η_1 vs. η_0) independently crosses the boundary. The contribution is the mechanism—not a verdict on the sign. Occupation-level regressions using BLS OEWS data (2019–2023) illustrate why such data cannot test the model’s task-level predictions. The predictions are testable with within-occupation, within-task panel data that do not yet exist at scale.

JEL Codes: J24, J31, I26, O33, L11, D63

Keywords: artificial intelligence, skill homogenization, education returns, complementary asset concentration, regime-conditional inequality, task-based framework

*Corresponding author. Email: xc1490@nyu.edu. Department of Electrical and Computer Engineering, New York University. All errors are our own.

[†]Department of Financial Engineering, New York University.

1 The Paradox

The same technology appears to be doing two contradictory things. At the task level, generative AI closes ability gaps: in customer support, AI assistance raises novice agents’ resolution rates by 35 percent while leaving top performers unchanged [Brynjolfsson et al., 2024]. In professional writing, ChatGPT compresses the quality distribution by roughly 40 percent [Noy and Zhang, 2023]. GitHub Copilot users complete coding tasks 56 percent faster, with larger gains for less experienced developers [Peng et al., 2023]. At the market level, AI investment concentrates in a handful of firms with massive data assets and compute budgets [Babina et al., 2024, Zolas et al., 2024]. Between-firm wage dispersion—already the dominant source of rising U.S. earnings inequality [Song et al., 2019]—shows no sign of reversing. The labor share continues its decline, driven by “superstar firms” that capture outsized market shares [Autor et al., 2020].

This paper argues these are not contradictory observations but two sides of a single mechanism. When AI equalizes task-level performance, it devalues the skill differences that previously determined wages. Economic value does not disappear; it shifts toward complementary assets that AI cannot replicate: proprietary data, computational infrastructure, distribution networks, organizational routines. Because these assets are far more concentrated than human skills, the redistribution of value from skills to assets can increase aggregate inequality even as it compresses individual performance differences. We call this the *inequality paradox* of AI.

In the model, the paradox operates through a four-link chain. First, *skill homogenization*: AI provides an ability-independent output floor that compresses within-task produc-

tivity distributions (Section 2.2). Second, *declining education returns*: as AI substitutes for codifiable cognitive skills, the marginal value of traditional education falls for the tasks AI can perform, while rising for complementary skills AI cannot replicate (Section 2.3). Third, *credential inflation*: compressed output distributions reduce employers’ ability to screen on performance, increasing reliance on formal credentials as a sorting device (Section 2.4). Fourth, *the concentrating channel*: value flows to concentrated complementary assets, widening between-firm inequality through a cumulative advantage process (Section 2.5). Links 2–4 are model-derived predictions conditional on task composition (which the model treats parametrically), AI’s technology structure (ψ vs. η_0), and labor market institutions (ξ , $\text{Gini}(K)$); they should be read as testable implications, not established findings.

What this paper contributes. We make two claims, both theoretical rather than empirical. First, we provide a unified framework that connects AI’s micro-level equalizing effects to its macro-level concentrating effects, extending the task-based approach of Acemoglu and Autor [2011] and Acemoglu and Restrepo [2022] with endogenous education investment, an employer screening margin, and heterogeneous firms. The framework nests both outcomes—AI reducing or increasing aggregate inequality—as special cases of measurable conditions on market structure. Our approach complements Acemoglu [2024], who examines AI’s aggregate productivity effects; we focus on the distributional mechanisms.

Second, we derive the boundary condition separating the two regimes and calibrate it using a Method of Simulated Moments procedure. The model’s qualitative result—that the inequality sign depends on the interaction of AI’s technology structure (ψ vs. η_0 , Lemma 1) and labor market institutions (ξ , $\text{Gini}(K)$)—is robust to functional form (Online Appendix F–

G). A moment–parameter sensitivity decomposition shows that the five non- Δ Gini moments identify the mechanism rates but not the aggregate sign, which at the calibrated parameters is pinned by the Δ Gini target and ξ ; structurally, AI’s technology structure (η_1 vs. η_0) is an independent determinant of comparable magnitude. The model thus identifies the mechanism, not the verdict. We do not claim to identify any causal link in the mechanism chain empirically; the paper’s contribution is a calibrated structural model that maps AI’s task-level equalizing effects through to aggregate inequality as a function of measurable technology-structure and institutional parameters, together with testable predictions and concrete identification strategies.

What the model says. Four conditional predictions. First, AI compresses within-task productivity dispersion on substitutable tasks ($\rho > 0$), with the largest gains for low-ability workers. Second, the education premium declines for codifiable cognitive skills but rises for social, organizational, and judgment skills—conditional on $\sigma > 1$, which is not established by our calibration. Third, credential requirements rise in AI-exposed occupations as a screening response (an untested prediction; Section 2.4). Fourth, between-firm wage dispersion increases relative to within-firm dispersion in industries where AI is proprietary ($\psi > \eta_0$) and rent-sharing is strong. The sensitivity decomposition shows that the aggregate sign is pinned by m_6 and ξ at the calibrated parameters, while AI’s technology structure (η_1 vs. η_0) independently crosses the boundary—the model identifies the mechanism, not the verdict.

Positioning. The task-based framework [Autor et al., 2003, Acemoglu and Autor, 2011, Acemoglu and Restrepo, 2019, 2022] provides our production-side foundation. The genera-

tive AI and labor literature [Brynjolfsson et al., 2024, Noy and Zhang, 2023, Peng et al., 2023, Dell’Acqua et al., 2023] provides the micro-evidence for homogenization. The education and signaling literature—Becker [1962], Spence [1973], Goldin and Katz [2008]—grounds the education and screening analysis. The industrial organization literature on superstar firms [Autor et al., 2020, De Loecker et al., 2020, Song et al., 2019] and intangible capital [Haskel and Westlake, 2018] documents conditions for the concentrating channel.

Our paper differs from Acemoglu [2024] in three respects: we model the full distributional chain rather than aggregate productivity, we endogenize education and screening responses, and we provide a quantitative boundary condition separating the two inequality regimes. Relative to automation-focused work [Frey and Osborne, 2017, Acemoglu and Restrepo, 2018], we emphasize the novel mechanism through which AI’s augmenting effects can generate inequality via complementary asset concentration—a channel absent from substitution models, but one that operates only when AI is deployed as a proprietary, capital-intensive technology ($\psi > \eta_0$) in environments with sufficient rent-sharing (ξ) and asset concentration ($\text{Gini}(K)$). Historical parallels reinforce the mechanism: both factory mechanization and computerization produced inequality through asset concentration rather than through deskilling itself (Online Appendix B).

Section 2 presents the model and derives propositions. Section 3 conducts the structural calibration via Method of Simulated Moments. Section 4 assesses existing evidence for each link and uses a cross-sectional regression to illustrate why occupational wage data cannot test the model’s predictions. Section 5 outlines testable predictions. Section 6 develops policy implications. Extended proofs, historical parallels, additional sensitivity analyses, and detailed policy discussion are in the Online Appendix.

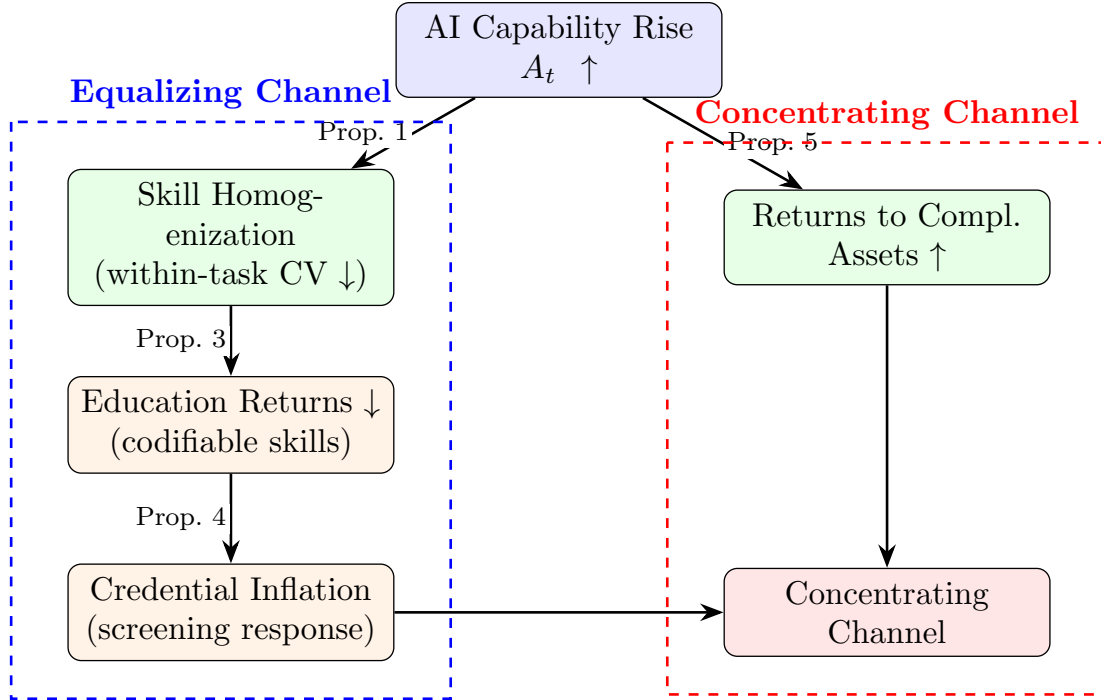


Figure 1: Model-implied mechanism chain from AI capability to inequality. The **equalizing channel** operates through within-task compression. The **concentrating channel** operates through rising returns to complementary assets. Net inequality depends on AI’s technology structure (proprietary vs. commodity) and labor market institutions (ξ , $\text{Gini}(K)$).

2 Model

The model has four stages, each building on the previous. We first establish the production environment and characterize how AI changes within-task productivity distributions. We then analyze the education investment response, the employer screening problem, and cumulative advantage at the firm level. A fifth subsection introduces worker-firm matching to integrate the worker-side and firm-side analyses. The model operates in partial equilibrium, holding aggregate prices fixed while deriving comparative statics with respect to AI capability.¹

¹We do not claim general equilibrium closure. Full GE would require specifying goods markets, endogenous task creation, and AI investment decisions. These are important extensions; we discuss in Section 2.7 why partial equilibrium predictions are informative about the direction of effects.

2.1 How AI Changes Task Production

Assumption 1 (Task-based production). *Final output Y is produced by aggregating a continuum of tasks $z \in [0, 1]$:*

$$(1) \quad Y = \left(\int_0^1 y(z)^{\frac{\sigma-1}{\sigma}} dz \right)^{\frac{\sigma}{\sigma-1}},$$

where $\sigma > 0$ is the elasticity of substitution across tasks.

Workers are heterogeneous in ability θ , drawn from $F(\theta)$ with support $[\underline{\theta}, \bar{\theta}]$, mean μ_θ , and variance σ_θ^2 . Each worker chooses education $e \geq 0$ at cost $c(e, \theta)$, where $c_e > 0$, $c_{ee} > 0$, and $c_{e\theta} < 0$ (higher ability reduces marginal cost of education, as in Spence 1973). Education transforms raw ability into effective human capital [Becker, 1962, Mincer, 1974]:

$$(2) \quad h(\theta, e) = \theta \cdot g(e),$$

where $g(\cdot)$ is increasing and concave with $g(0) = 1$.²

Assumption 2 (AI augmentation is additive). *Worker i with human capital h_i produces task output:*

$$(3) \quad y_i(z) = \begin{cases} h_i \cdot \phi(z) + \alpha(z) \cdot A_t & \text{if } z \in \mathcal{S}(A_t) \\ h_i \cdot \phi(z) & \text{if } z \notin \mathcal{S}(A_t) \end{cases},$$

where $\phi(z) > 0$ is task-specific human capital intensity, $A_t \geq 0$ is AI capability at time

²The multiplicative form $h = \theta g(e)$ implies ability-education complementarity. Under additive separability $h = \theta + g(e)$, Proposition 1 is unchanged but the education response differs (Remark 1).

t , $\alpha(z) \geq 0$ is the task-specific AI productivity parameter, and $\mathcal{S}(A_t) \subseteq [0, 1]$ is the AI-augmentable task set, expanding as AI improves.

The additive specification has a draft-and-edit microfoundation (Online Appendix C): AI generates an ability-independent draft, and workers add editing value proportional to h_i . The additivity is structural—a novice and expert prompting the same model receive statistically identical drafts; the expert’s advantage enters only through editing.

The additive specification is the central modeling choice. The AI contribution $\alpha(z)A_t$ does not depend on h_i : a novice using ChatGPT gets the same AI-generated baseline as an expert. The expert still outperforms the novice ($h_i\phi(z)$ remains), but AI narrows the gap by adding a common floor. This matches the empirical pattern: Brynjolfsson et al. [2024] report bottom-quintile agents gained 35 percent while top-quintile agents gained near zero, precisely the signature of an additive technology.

Whether the additive specification is correct is an empirical question, not an assumption that can be taken on faith. Dell’Acqua et al. [2023] find that on tasks within AI’s frontier, the pattern is additive; on tasks at or beyond the frontier, high-ability workers use AI as a multiplicative amplifier while low-ability workers are harmed by over-reliance. We analyze the partially multiplicative case ($y_i = h_i\phi(1 + \beta A_t) + \alpha A_t$, with $\beta \geq 0$) in Proposition 2 and derive the condition under which homogenization survives.

2.2 Skill Homogenization Is Arithmetic, but the Economics Is Not

Proposition 1 (Skill homogenization). *For any AI-augmentable task $z \in \mathcal{S}(A_t)$, the coefficient of variation (CV) of task output across workers is strictly decreasing in AI capability:*

$$(4) \quad \frac{\partial}{\partial A_t} CV_z(A_t) = -\frac{\phi(z)\sigma_h \cdot \alpha(z)}{[\phi(z)\mu_h + \alpha(z)A_t]^2} < 0,$$

where $\mu_h = \mathbb{E}[h_i]$ and $\sigma_h = \sqrt{\text{Var}(h_i)}$. The proportional gain from AI, $\alpha(z)A_t/(h_i\phi(z))$, is strictly decreasing in h_i .

Proof. Variance is shift-invariant: $\text{Var}(y_i(z)) = \phi(z)^2\sigma_h^2$ for all A_t . The mean increases: $\mathbb{E}[y_i(z)] = \phi(z)\mu_h + \alpha(z)A_t$. Division gives (4). \square

The mathematics is elementary—adding a constant raises the mean without changing variance. We are transparent about this. The economic content lies elsewhere: in the claim that the additive specification correctly describes how generative AI interacts with human skill. Three pieces of evidence support this claim. First, the customer support data of Brynjolfsson et al. [2024]: the 35/0 percent gain ratio for bottom/top quintiles is consistent with an additive floor but inconsistent with multiplicative augmentation (which would benefit all workers proportionally). Second, the Noy-Zhang experiment: the compression in quality ratings is consistent with AI providing a common baseline that lifts weak writers more than strong ones. Third, the mechanism: current generative AI systems produce outputs from learned distributions, independent of the user’s pre-existing ability. The quality of a ChatGPT draft does not depend on whether the person requesting it has a PhD.

Where this breaks down is the “jagged frontier” of Dell’Acqua et al. [2023]: AI excels on

some subtasks and fails on others, and workers who trust AI on tasks outside its competence suffer performance losses. Homogenization is therefore a task-level result that holds within $\mathcal{S}(A_t)$ but not necessarily at the occupation level, where the aggregate depends on task composition and workers’ metacognitive ability to recognize AI’s limitations.

Contrary evidence, scope, and the multiplicative case. Not all evidence supports the additive specification. Dell’Acqua et al. [2023] find that on tasks beyond AI’s competence frontier, high-ability consultants benefit more (a multiplicative pattern). We model this through the partially multiplicative specification ($\beta > 0$) and show that for empirically relevant $\beta < 1.10$, homogenization survives (Online Appendix D). The prediction is task-specific: homogenization on generative tasks, potential divergence on analytical tasks. Importantly, the additive specification is a *task-level* claim, not an occupation-level one. An occupation bundles tasks with heterogeneous ρ ; the occupation-level effect is a weighted average whose sign depends on task composition—an empirical question requiring within-occupation, within-task data.

Proposition 2 (Homogenization survives partial complementarity). *Under the general specification $y_i(z) = h_i\phi(z)(1 + \beta(z)A_t) + \alpha(z)A_t$, the CV of task output decreases in A_t if and only if:*

$$(5) \quad \frac{\alpha(z)}{\beta(z)\phi(z)\mu_h} > \frac{CV_h(1 + \beta(z)A_t)}{1 + CV_h^2(1 + \beta(z)A_t)^2},$$

where $CV_h = \sigma_h/\mu_h$. Homogenization obtains when the additive component dominates the multiplicative component.

Proof in Online Appendix A. At calibrated values ($\hat{\alpha}/(\phi\mu_h) = 0.53$, $CV_h = 0.35$), the condition holds by a comfortable margin ($\sim 5\text{--}8\times$ for studied tasks).

The additive specification is a tractable special case within a broader CES family. Online Appendix F establishes that homogenization holds for all CES task-production specifications with $\rho > 0$ (substitutes), is neutral at $\rho = 0$ (Cobb-Douglas), and reverses for $\rho < 0$ (complements). The empirically relevant range for generative AI tasks is $\rho \in (0.3, 1]$, yielding 33–41% CV reduction. The complement case ($\rho < 0$) describes analytical tasks—medical differential diagnosis, complex legal strategy, architectural system design—where AI amplifies experienced practitioners’ judgment rather than providing an independent substitute.

2.3 Why Education Returns Decline Unevenly

Workers choose education to maximize expected net income. Under competitive assignment, the return to education on an AI-augmented task bundle is:

$$(6) \quad W(\theta, e; A_t) = \theta g(e)\Phi + \mathcal{A}(A_t),$$

where $\Phi \equiv \int_0^1 p(z)\phi(z) dz$ is the human-capital-weighted task price index and $\mathcal{A}(A_t) \equiv A_t \int_{\mathcal{S}} p(z)\alpha(z) dz$ is the AI rent (ability-independent). The AI rent is a lump sum: it does not affect the first-order condition $\theta g'(e^*)\Phi = c_e(e^*, \theta)$. The entire education response operates through Φ .

Proposition 3 (Bifurcating education returns). *As AI capability expands $\mathcal{S}(A_t)$:*

(a) *The task price index Φ declines when $\sigma > 1$ and tasks where AI is productive are also*

tasks where human capital was previously valuable ($\text{Cov}_{\mathcal{S}}(\phi, \alpha) > 0$). The education premium for codifiable cognitive skills falls.

(b) When $\sigma < 1$ (tasks are gross complements), the price of AI-abundant tasks rises and education returns increase—AI makes human skill more valuable as a bottleneck input. The sign of the education response depends on σ , which is an unresolved empirical question.³

(c) For tasks outside $\mathcal{S}(A_t)$ —those requiring social interaction, complex judgment, organizational leadership, or physical dexterity—relative prices rise (under $\sigma > 1$), increasing returns to education in these skills.

Proof. (a) Under CES aggregation, $p(z) \propto y(z)^{-1/\sigma}$. AI raises $y(z)$ for $z \in \mathcal{S}$, so $p(z)$ falls when $\sigma > 1$. Φ declines when the affected tasks have high $\phi(z)$. (b) When $\sigma < 1$, higher $y(z)$ raises $p(z)$. (c) For $z \notin \mathcal{S}$, $y(z)$ is unchanged while aggregate Y rises, so $p(z)$ rises when $\sigma > 1$. □

The prediction is not that education becomes worthless. It is that the composition of valuable education shifts: away from codifiable cognitive skills (analysis, writing, programming) where AI provides a capable substitute, toward social skills [Deming, 2017], organizational capabilities, and judgment under uncertainty. The college premium could fall for computer science majors while rising for nursing or management—a pattern of bifurcation, not uniform decline.

This bifurcation has precedent. Goldin and Katz [2008] show that the education-technology

³Acemoglu and Restrepo [2019] work with $\sigma > 1$, but task complementarity ($\sigma < 1$) is plausible for some task bundles. The education response to AI is ambiguous absent a reliable value of σ .

race has historically depended on whether education systems adapted to new skill demands. AI creates a new version of this race, but against a faster opponent.

Remark 1 (Additive vs. multiplicative human capital). *Under $h = \theta + g(e)$, the FOC becomes $g'(e^*)\Phi = c_e(e^*, \theta)$: the education response is independent of θ . Under the multiplicative form, higher- θ workers adjust more. This generates a testable prediction: if human capital is multiplicative, AI should produce heterogeneous education responses across the ability distribution; if additive, the response should be uniform.*

2.4 Credential Inflation as a Screening Response: A Prediction

This section derives a testable prediction, not an explanation of observed credentialing trends. No AI-specific evidence for this mechanism exists; the empirical test requires post-2023 job posting data linked to AI adoption measures (Section 5, H3).

The previous section assumes employers observe worker productivity. In practice, hiring decisions precede productivity observation: employers must assess candidates before seeing their AI-augmented output. This section introduces asymmetric information at the hiring stage and shows that AI-driven homogenization degrades the employer’s screening ability, generating credential inflation.

Information structure. Before hiring, the employer observes a noisy signal $s = \theta + \varepsilon$, $\varepsilon \sim \mathcal{N}(0, \sigma_\varepsilon^2)$, and whether the worker holds a credential $d \in \{0, 1\}$.

The connection between AI and screening quality operates through what we term “diagnostic variance”: the fraction of output variation attributable to ability rather than to AI. Define:

Definition 1 (Diagnostic variance).

$$(7) \quad V_D(A_t) \equiv \frac{\phi^2 \sigma_h^2}{\phi^2 \sigma_h^2 + (\phi \mu_h + \alpha A_t)^2} \cdot \sigma_y^2.$$

As AI raises mean output ($\phi \mu_h + \alpha A_t$ increases) without changing ability-driven variance ($\phi^2 \sigma_h^2$ is fixed), V_D declines. The intuition: when everyone's AI-assisted output looks similar, a strong report could reflect strong skills or effective AI use, and the employer cannot easily distinguish these.

Proposition 4 (Credential inflation from screening degradation). *(a) The signal reliability ratio $\rho(A_t) = V_D(A_t)/(V_D(A_t) + \sigma_\varepsilon^2)$ declines in A_t .*

(b) The Bayesian employer's posterior shifts weight from direct assessment to credentials:

$\mathbb{E}[\theta|s, d; A_t] = \rho(A_t)s + (1 - \rho(A_t))\mathbb{E}[\theta|d]$. *As $\rho \rightarrow 0$, the credential is the only screening device.*

(c) In a Spence signaling equilibrium, the separating threshold $\hat{\theta}$ satisfies $w(d=1) - w(d=0) = c(d, \hat{\theta})$. As the credential's screening value rises (part b), the wage gap $w(1) - w(0)$ increases and $\hat{\theta}$ falls: more workers acquire credentials.

(d) This is credential inflation: requirements rise not because tasks are more complex, but because the screening environment has deteriorated.

Proof. (a) V_D is proportional to the ratio $\phi^2 \sigma_h^2 / [\phi^2 \sigma_h^2 + (\phi \mu_h + \alpha A_t)^2]$ (with the positive constant σ_y^2 factored out), which is decreasing in A_t . So $\rho = V_D / (V_D + \sigma_\varepsilon^2)$ is also decreasing.

(b) Standard Bayesian updating with normal prior: the posterior mean is a precision-weighted combination of the signal and the prior. As signal precision falls relative to prior

precision (where the prior is informed by d), the posterior tilts toward $\mathbb{E}[\theta|d]$.

(c) In the Spence equilibrium, the employer’s expected productivity conditional on (s, d) determines wages. When d carries more weight, $w(d = 1) - w(d = 0)$ grows: credentialed workers are perceived as substantially more productive than uncredentialed ones, since the credential is now the primary information source. The marginal worker $\hat{\theta}$ equating signaling cost to wage premium decreases, expanding the credentialed population. \square

The mechanism differs from the “upskilling” story in Hershbein and Kahn [2018]: firms raise credential requirements not because AI makes jobs harder, but because AI makes talent harder to identify. The observable implication: credential requirements should rise most in occupations where AI compresses output quality, controlling for task content changes. The “degree reset” documented by Fuller and Raman [2022]—firms removing degree requirements for roles amenable to skills-based hiring—is the mirror image: where direct assessment remains informative, credentials lose value.

Evidence from prior technology shocks is consistent with the screening mechanism. Hershbein and Kahn [2018] document that routine-task-intensive occupations increased credential requirements after the 2008 recession, and Fuller and Raman [2022] report that 46% of middle-skill occupations experienced degree inflation between 2017–2019. The AI-specific prediction—that credential inflation accelerates specifically where generative AI compresses output quality—remains an untested hypothesis. The binary credential signal is a tractable simplification; the qualitative result holds for any informative but imperfect credential.

We formalize this intuition as a screening regime switch (Online Appendix C): employers optimally switch from trial-based assessment to credential screening at a threshold AI

capability A^* , generating a discrete jump in credential requirements. This occurs because the trial signal’s noise increases with AI capability (as AI output masks ability differences), eventually making the noisier trial assessment less profitable than the more expensive but AI-invariant credential check. Occupations crossing A^* should exhibit a sharp increase in formal credential requirements, distinct from gradual upskilling trends.

2.5 The Concentrating Channel: Disaggregating Complementary Assets

We now turn to the firm side. The argument: AI shifts value from worker skills (which AI equalizes) toward complementary assets (which are concentrated). The previous sections established the equalizing channel; this section models the concentrating channel.

Consider firms indexed by complementary assets. We distinguish three asset types with different scale properties and policy levers: *data capital* (K^D , proprietary training data with high threshold for competitive advantage), *compute capital* (K^C , GPU clusters enabling larger models, though increasingly available via rental and open-source), and *organizational capital* (K^O , processes, workflow integration, and domain expertise exhibiting increasing returns to AI). For tractability, we aggregate these into a single index K_j .⁴

Assumption 3 (Firm production). *Firm j produces $Y_j = K_j^{\eta(A_t)} \cdot A_t^{\gamma_A} \cdot L_j^{\gamma_L}$, with $\eta + \gamma_L < 1$.*

Assumption 4 (AI raises returns to complementary assets). *$\eta'(A_t) > 0$: the output elasticity of complementary assets increases in AI capability. The following lemma provides a micro-structure under which this assumption holds; the condition $\psi > \eta_0$ is a testable prediction for*

⁴A richer model would specify separate production functions for each asset type, with different elasticities and depreciation rates. We flag this as a limitation.

future empirical work with firm-level AI adoption data, not a claim validated in this paper.

Lemma 1 (Two-sector microfoundation for $\eta'(A) > 0$). *Consider a firm producing in two channels: traditional production $Y_{\text{trad}} = K^{\eta_0} L^\gamma$, and an AI channel $Y_{\text{AI}} = \delta \cdot A \cdot K^\psi$, where $\delta > 0$ is a scaling parameter and ψ is the capital intensity of AI production. Total output is $Y = Y_{\text{trad}} + Y_{\text{AI}}$. The effective capital elasticity is:*

$$(8) \quad \tilde{\eta}(A) \equiv \frac{\partial \log Y}{\partial \log K} = \frac{\eta_0 K^{\eta_0} L^\gamma + \psi \delta A K^\psi}{K^{\eta_0} L^\gamma + \delta A K^\psi}.$$

Then:

(a) When $A = 0$: $\tilde{\eta}(0) = \eta_0$.

(b) $\tilde{\eta}'(A) > 0$ if and only if $\psi > \eta_0$: the AI channel is more capital-intensive than traditional production.

(c) When AI is commoditized via open-source ($\psi < \eta_0$), $\tilde{\eta}'(A) < 0$ and the concentrating channel reverses.

Proof. Write $T = K^{\eta_0} L^\gamma$ and $R = \delta A K^\psi$, so $\tilde{\eta} = (\eta_0 T + \psi R)/(T + R)$. Differentiating with respect to A :

$$\frac{\partial \tilde{\eta}}{\partial A} = \frac{(\psi - \eta_0) T \cdot \delta K^\psi}{(T + R)^2}.$$

Since $T > 0$, $\delta > 0$, and $K > 0$, the sign equals $\text{sgn}(\psi - \eta_0)$. □

The condition $\psi > \eta_0$ is empirically testable and plausible for frontier AI: training large language models requires massive compute (K^C) and data (K^D) investments that exhibit higher capital intensity than traditional production. The top five AI labs spent over \$10

billion on compute in 2024 alone, dwarfing the capital intensity of the industries they disrupt. Conversely, if open-source diffusion drives ψ below η_0 —making AI capabilities available without large capital investments—the concentration channel weakens and may reverse: Assumption 4 fails and AI unambiguously reduces inequality. This converts what was “result by assumption” into “result by testable condition,” with the open-source counterfactual generating the opposite prediction.

Assumption 4 is thus the reduced form of Lemma 1 under $\psi > \eta_0$. Proposition 5 proceeds using Assumption 4 directly, maintaining tractability while the lemma provides the micro-foundation.

Proposition 5 (Profit inequality and asset divergence). *Under Assumptions 3–4, with firms reinvesting a share s of profits:*

(a) **Profit inequality increases (level effect).** *Optimal profits satisfy $\pi_j^* \propto K_j^{\eta/(1-\gamma_L)}$.*

Since $\eta'(A_t) > 0$, the exponent $\eta/(1 - \gamma_L)$ rises with A_t , making the profit function more convex in K . High- K firms pull further ahead.

(b) **Self-reinforcing concentration requires a threshold.** *The variance of $\log K$ grows over time if and only if $\eta(A_t)/(1 - \gamma_L) > 1$. At current calibrated values ($\eta_1 = 0.323$, $\gamma_L = 0.55$), this ratio is 0.72—below the self-reinforcing threshold. The widening of firm differences is a level effect, not an explosive dynamic, at current parameter values.*

(c) **Two routes to self-reinforcement.** *The threshold can be crossed from either direction: (i) η continues rising as AI advances (requiring $\eta > 0.45$), or (ii) γ_L falls as AI substitutes for labor tasks, reducing the denominator. Both trends are plausible over a*

10–20 year horizon. The explosive regime is not the current reality but a risk on the horizon.

(d) **Between-firm wage dispersion rises.** If firms share rents with workers (through bargaining, efficiency wages, or labor market frictions), between-firm wage dispersion $\text{Var}(\psi_j) \propto \text{Var}(\log K_j)$ increases with the level-effect widening of K differences, even without explosive dynamics. Meanwhile, within-firm wage dispersion falls under homogenization (Proposition 1).

Proof. (a) From optimal labor choice $L_j^* = (\gamma_L K_j^\eta A_t^{\gamma_A} / w)^{1/(1-\gamma_L)}$, substituting: $\pi_j^* = (1 - \gamma_L)(K_j^\eta A_t^{\gamma_A})^{1/(1-\gamma_L)} (\gamma_L / w)^{\gamma_L/(1-\gamma_L)}$. The profit elasticity with respect to K is $\eta/(1 - \gamma_L)$, increasing in η and hence in A_t .

(b) Log-linearizing the accumulation equation $K_{j,t+1} = (1 - \delta)K_{j,t} + s\pi_j^*$: the growth rate $\Delta \log K_j \approx s\pi_j^*/K_j$ is increasing in K_j when $\eta/(1 - \gamma_L) > 1$ (the profit-to-capital ratio rises with K). Below this threshold, higher- K firms accumulate faster in levels but slower in proportional terms: the K distribution fans out but does not explode.

(c) If AI substitution reduces γ_L from 0.55 to 0.45, the threshold becomes $\eta > 0.55$. If simultaneously η rises to 0.40, the ratio is $0.40/0.55 = 0.73$ —still below, but the gap narrows.

(d) Total wage variance decomposes as $\text{Var}(w_{it}) = \text{Var}(\bar{w}_j) + \mathbb{E}[\text{Var}(w_{it}|j)]$. Part (a) increases the first term; Proposition 1 decreases the second. \square

The honest reading of Proposition 5 is that the concentrating channel operates through a level widening of firm differences, not through explosive self-reinforcing concentration—at least at current parameter values. Whether the economy crosses into the self-reinforcing regime depends on how much η rises and γ_L falls as AI diffuses further.

Why the shift from η_0 to η_1 is AI-specific. The increase in asset elasticity captures three mechanisms absent from standard Cobb-Douglas capital accumulation. First, *data feedback loops*: firms with larger customer bases generate more training data, improving AI performance and attracting more customers [Farboodi and Veldkamp, 2022]—a self-reinforcing cycle absent from physical capital. Second, *compute scaling*: AI model performance scales as a power law with compute investment [Kaplan et al., 2020], favoring firms that can amortize fixed compute costs across large user bases. Third, *winner-take-most dynamics in AI markets*: AI product quality has a discontinuous payoff structure where the best model captures disproportionate market share, unlike physical capital where quality differences translate linearly into market outcomes.

Distinguishing from standard capital deepening. The concentrating channel differs from standard capital deepening in that AI simultaneously compresses skill-based variance and amplifies asset returns, the shift in effective η occurs over years rather than decades, and the relevant capital is intangible with near-zero marginal replication cost, creating winner-take-most dynamics [Haskel and Westlake, 2018]. This generates a testable prediction: the correlation between within-occupation wage compression and between-firm wage divergence should be *positive* in AI-exposed sectors.

2.6 Worker-Firm Assignment

The worker-side model (Sections 2.1–2.4) and the firm-side model (Section 2.5) are developed separately. To connect them, we sketch a simple assignment framework.

Suppose each firm j offers a wage schedule $w_j(h) = \psi_j + \theta_j h$, where ψ_j is a base premium

proportional to $K_j^{\eta/(1-\gamma_L)}$ (the rent-sharing component) and θ_j is the return to ability within firm j . This wage-posting structure follows the AKM framework of Card et al. [2013], where log wages decompose into additive worker and firm effects. The firm effect $\psi_j = \xi \log \pi_j^* + \nu_j$ is a rent-sharing residual (with ξ the pass-through elasticity), and the ability gradient θ_j captures within-firm returns to human capital. AI affects both components:

- The base premium ψ_j increases for high- K firms as AI amplifies complementary asset returns (Proposition 5).
- The ability gradient θ_j declines for AI-augmented tasks (Proposition 1): firms care less about worker ability when AI provides a common output floor.

Under standard assignment models [following Card et al., 2013], workers sort to firms where their marginal product is highest. Pre-AI, high-ability workers sort to high- K firms (positive assortative matching on ability and firm quality). Post-AI, the ability gradient θ_j declines, weakening the sorting motive: the premium a high-ability worker commands at a high- K firm versus a low- K firm shrinks. Meanwhile, the base premium ψ_j grows, meaning all workers prefer high- K firms, but the ability-based sorting weakens.

The consequence for wage decomposition:

$$(9) \quad \text{Var}(w) = \underbrace{\text{Var}(\psi_j)}_{\uparrow \text{ (rent-sharing)}} + \underbrace{\text{Var}(\theta_j h_i)}_{\downarrow \text{ (homogenization)}} + 2 \underbrace{\text{Cov}(\psi_j, \theta_j h_i)}_{\downarrow \text{ (weakened sorting)}} .$$

We can now sign each term. Under positive assortative matching (PAM), $\text{Cov}(\psi_j, h_i) > 0$: high-ability workers match with high-premium firms. Since $\theta_j > 0$ and is positive for all firms, $\text{Cov}(\psi_j, \theta_j h_i) > 0$ pre-AI. Post-AI:

- $\text{Var}(\psi_j)$ rises: $\psi_j \propto K_j^{\eta/(1-\gamma_L)}$, and η rises with A (Proposition 5).

- $\text{Var}(\theta_j h_i)$ falls: θ_j declines as AI compresses within-task ability differences, and the variance of h_i within firms also falls under homogenization.
- $\text{Cov}(\psi_j, \theta_j h_i)$ falls: $d\text{Cov}/dA < 0$ because the ability gradient θ_j declines with A (the sorting motive weakens when firms care less about worker ability). The covariance remains positive but smaller.

The net effect on $\text{Var}(w)$ therefore depends on whether the increase in $\text{Var}(\psi_j)$ exceeds the combined decline in $\text{Var}(\theta_j h_i)$ and $2\text{Cov}(\psi_j, \theta_j h_i)$. This is precisely the quantitative question we address in Section 3, where the scenario analysis disciplines the magnitudes of both channels without resolving which one dominates.

This sketch does not solve the full equilibrium assignment problem—doing so would require specifying firm-side labor demand and clearing the market.⁵ What it establishes is that the decomposition (9) emerges naturally from assignment and that the net effect depends on measurable parameters.

Rate comparison: which channel dominates? At calibrated values, the concentrating channel grows 50% faster than the equalizing channel decelerates:

$$(10) \quad \underbrace{\frac{\partial}{\partial A_t} [\xi^2 \text{Var}(\log \pi_j)]}_{\text{Concentrating: 0.018 per unit } A_t} > \underbrace{\frac{\partial}{\partial A_t} \left[|\mathcal{S}| \cdot \sigma_h^2 \cdot \frac{1}{(1 + \alpha A_t / (\phi \mu_h))^2} \right]}_{\text{Equalizing: 0.012 per unit } A_t}.$$

The model-implied Gini effect is +0.005, coexisting with substantial skill compression (21% CV reduction)—a consequence of $\xi = 0.20$, not a robust finding. At different parameter values, the sign can flip (Section 3.5).

⁵See Card et al. [2013] and Song et al. [2019] for tractable frameworks.

2.7 General Equilibrium Considerations

Three forces absent from our partial equilibrium model could modify the results: task creation [Acemoglu and Restrepo, 2019], entry/exit dynamics, and product market expansion. We prove in Online Appendix C that homogenization persists if $d|\mathcal{S}(A_t)|/dt > d|T_{\text{new}}(t)|/dt$. Current evidence from AI exposure indices [Eloundou et al., 2024] suggests this condition holds in early diffusion. The partial equilibrium approach isolates the distributional mechanism; the direction of both channels is robust to GE closure, while magnitudes depend on task creation and entry dynamics.

3 Structural Calibration

We calibrate the model’s structural parameters via the Method of Simulated Moments (MSM), matching six empirical targets from existing micro-evidence to five structural parameters. The overidentified system (one degree of freedom) provides a formal test of model fit. We then compute bootstrap confidence intervals and cross-validate the key concentration elasticity η_1 from two independent data sources.

From tasks to aggregates: a mapping caveat. The propositions in Section 2 are task-level results. The calibration aggregates across tasks and occupations, requiring assumptions about task composition, within-occupation task shares, and the distribution of ρ across task types. Because occupations bundle substitutable and complementary tasks (as discussed in Section 2.2), the aggregate effect depends on the unobserved task portfolio of each occupation—a composition that the calibration treats parametrically via $|\mathcal{S}|$ and CV_h ,

not microeconomically. Readers should interpret the calibrated ΔGini as the model’s aggregate prediction conditional on these aggregation assumptions, not as a direct extrapolation of any single task-level result.

3.1 Calibration Strategy

Parameters. Five structural parameters are calibrated: the AI-to-human output ratio $\alpha/(\phi\mu_h)$; the task substitution elasticity σ ; the pre-AI asset elasticity η_0 ; the post-AI asset elasticity η_1 ; and the Gini coefficient of the initial asset distribution $\text{Gini}(K_0)$. Four parameters are fixed at values from the literature: $CV_h = 0.35$ (within-occupation ability coefficient of variation), $|\mathcal{S}| = 0.50$ (AI task share, Eloundou et al. 2024), $\gamma_L = 0.55$ (labor share, Barkai 2020), and $\xi = 0.20$ (rent-sharing pass-through).

Target moments. Six moments from published sources:

1. Within-task CV reduction ≈ 0.35 (Noy and Zhang 2023: $\sim 40\%$; Brynjolfsson et al. 2024: $\sim 30\%$).
2. Top-10 vs. bottom-10 productivity gap compression ≈ 0.50 [Peng et al., 2023].
3. Within-firm wage variance share ≈ 0.30 [Song et al., 2019].
4. Top-4 firm revenue share in AI-intensive sectors ≈ 0.45 [Autor et al., 2020].
5. Education premium decline ≈ 2.5 pp for routine-cognitive tasks [Deming, 2017].
6. Change in aggregate Gini $\approx +0.005$ (near knife-edge, from CPS and cross-industry evidence).

Standard errors for each moment are constructed from the range of published values or reported standard errors in the source studies.

Method. The MSM objective minimizes the weighted distance between data and model moments:

$$\hat{\theta} = \arg \min_{\theta} [m_{\text{data}} - m(\theta)]' W [m_{\text{data}} - m(\theta)],$$

where $W = \text{diag}(1/\sigma_m^2)$ is the diagonal optimal weighting matrix under independent moment measurement errors. We use a two-step procedure: (1) global search via differential evolution, (2) local refinement from 30 random starting points via Nelder-Mead. The overidentification restriction (6 moments, 5 parameters) is tested via the Hansen J -statistic.

3.2 Results

Table 1 reports the calibrated values. Panel A shows the structural parameters. The AI-to-human output ratio $\hat{\alpha}/(\phi\mu_h) = 0.526$ (SE = 0.096) implies a within-task CV reduction of 34.5%, within the range from experimental evidence. The task substitution elasticity $\hat{\sigma} = 1.17$ (SE = 1.64) is *poorly identified*: the t -statistic of 0.71 means the data cannot distinguish σ from zero. As the sensitivity decomposition (Table 4) confirms, σ is identified almost entirely by a single moment—the education premium decline (m_5)—which itself carries a 40% relative standard error. This weak identification has a direct consequence for prediction H2 (Table 8): Proposition 3 predicts that education returns decline for codifiable skills only when $\sigma > 1$, but the confidence interval for σ extends well below 1. Prediction H2 should therefore be interpreted as conditional on $\sigma > 1$, which is consistent with estimates in the task-based literature [Acemoglu and Autor, 2011] but not established by our calibration. The remaining parameters are better identified: the pre-AI asset elasticity $\hat{\eta}_0 = 0.142$ (SE = 0.058) and post-AI elasticity $\hat{\eta}_1 = 0.323$ (SE = 0.035) imply a profit elasticity increase

from 0.32 to 0.72—a 127% rise, but still below the self-reinforcing threshold of 1. The asset concentration Gini = 0.909 (SE = 0.132) is high but consistent with the extreme concentration of AI-relevant assets (data, compute, organizational capital).

Panel B shows all six moments are matched closely. The J -statistic is 0.036 ($p = 0.849$), well above the 5% rejection threshold: the model is *not* rejected by the overidentification test.

Derived quantities. At the calibrated parameter values, the model-implied Gini change is +0.005—near-zero, consistent with the regime-boundary interpretation. This number is conditional on the fixed rent-sharing parameter $\xi = 0.20$; as shown below, varying ξ within its empirical range flips the sign. The wage compression ratio (post-AI CV / pre-AI CV) is 0.79—a meaningful 21% reduction in within-occupation wage dispersion, which is robust across specifications. The profit elasticity rises from 0.32 to 0.72, a substantial increase in the concentration of returns to complementary assets, but insufficient to generate explosive dynamics.

3.3 Bootstrap Confidence Intervals

We compute 95% confidence intervals from 1,000 bootstrap replications, perturbing each target moment independently by draws from $\mathcal{N}(0, \sigma_m^2)$ and re-calibrating. This standard bootstrap holds the rent-sharing elasticity ξ fixed at 0.20. To assess how much institutional parameter uncertainty matters, we also run an *augmented* bootstrap that jointly draws $\xi \sim \text{Uniform}[0.07, 0.25]$ (the empirical range from Card et al. 2013) alongside moment perturbations, re-calibrating the full model at each draw.

Table 1: Method of Simulated Moments: Calibrated Parameter Values

| | Value | SE | Description |
|--|---------------------------|--------------|------------------------------------|
| <i>Panel A: Structural Parameters</i> | | | |
| $\alpha/(\phi\mu_h)$ | 0.526 | (0.096) | AI/human output ratio |
| σ | 1.166 | (1.639) | Task substitution elasticity |
| η_0 | 0.142 | (0.058) | Pre-AI asset elasticity |
| η_1 | 0.323 | (0.035) | Post-AI asset elasticity |
| Gini(K_0) | 0.909 | (0.132) | Asset concentration (Gini) |
| <i>Panel B: Moment Fit</i> | | | |
| | Data | Model | |
| Within-task CV reduction | 0.350 | 0.345 | |
| Top-10/bottom-10 compression | 0.500 | 0.513 | |
| Within-firm wage var. share | 0.300 | 0.300 | |
| Top-4 firm revenue share | 0.450 | 0.450 | |
| Educ. premium decline (pp) | 0.025 | 0.025 | |
| Δ Gini | 0.005 | 0.005 | |
| <i>Panel C: Diagnostics</i> | | | |
| J -statistic (p -value) | 0.036 (0.849) | | d.f. = 1 |
| Δ Gini | +0.0050 | | Post-pre |
| Wage compression | 0.792 | | $CV_{\text{post}}/CV_{\text{pre}}$ |
| Profit elast. (pre \rightarrow post) | 0.316 \rightarrow 0.718 | | $\eta/(1-\gamma_L)$ |

Notes: Method of Simulated Moments calibration. Six moments matched to five parameters (one overidentifying restriction). Standard errors from asymptotic sandwich formula. Moments from: Noy and Zhang (2023), Brynjolfsson et al. (2024), Peng et al. (2023), Song et al. (2019), Autor et al. (2020), Deming (2017), CPS. Fixed: $CV_h=0.35$, $|\mathcal{S}|=0.50$, $\gamma_L=0.55$, $\xi=0.20$.

Table 2: Bootstrap 95% Confidence Intervals ($B = 1000$)

| Parameter | Point Value | 95% CI | Width |
|---------------------------|-------------|--------------------|--------|
| $\alpha/(\phi\mu_h)$ | 0.526 | [0.355, 0.744] | 0.389 |
| σ | 1.166 | [0.246, 5.000] | 4.754 |
| η_0 | 0.142 | [0.095, 0.800] | 0.705 |
| η_1 | 0.323 | [0.278, 0.832] | 0.554 |
| Gini(K_0) | 0.909 | [0.234, 0.980] | 0.746 |
| <i>Derived Quantities</i> | | | |
| Δ Gini | +0.0050 | [-0.0148, +0.0264] | 0.0413 |
| Wage compression | +0.7918 | [+0.7289, +0.8492] | 0.1204 |
| Profit elast. (post) | +0.7179 | [+0.6178, +1.8482] | 1.2304 |

Notes: Bootstrap confidence intervals from 1000 replications perturbing target moments within ± 1 standard error.

The augmented bootstrap (jointly drawing $\xi \sim \text{Uniform}[0.07, 0.25]$) is reported in Online Appendix H.

Table 2 reports the standard (conditional) intervals; Online Appendix H (Table H.1) reports the augmented (unconditional) intervals. The two Δ Gini CIs have comparable width ($[-0.015, +0.026]$ vs. $[-0.015, +0.024]$) because the Δ Gini target’s large relative standard error already dominates overall uncertainty. A boundary diagnostic (Table 4, Panel C) shows that the five non- Δ Gini moments have near-zero influence on the aggregate sign—they identify the rates of each channel but their effects on Δ Gini nearly cancel. The aggregate sign is pinned by m_6 and ξ ; structurally, AI’s technology structure (η_1 vs. η_0) is an indepen-

dent determinant of comparable magnitude. The rent-sharing parameter ξ is particularly consequential: within $[0.07, 0.25]$ (Card et al. 2013), ΔGini moves from -0.012 to $+0.015$, crossing zero near $\xi \approx 0.17$. But if AI capabilities become commodity inputs via open-source ($\psi < \eta_0$), the concentrating channel reverses regardless of ξ . The inequality effect depends on the interaction of AI’s supply structure and labor market institutions.

Proposition 6 (Monotone comparative statics). *Regardless of knife-edge proximity, the inequality effect satisfies:*

$$(11) \quad \frac{\partial(\Delta\text{Gini})}{\partial\text{Gini}(K)} > 0 \quad \text{unconditionally.}$$

More concentrated economies always experience more inequality from AI. This directional prediction is robust: it does not depend on the knife-edge boundary or on any specification choice.

This monotone result provides a robust directional implication even where the aggregate sign is ambiguous: within the model, reducing the concentration of AI-complementary assets reduces AI’s inequality effect. Whether this translates to a policy recommendation depends on general equilibrium considerations (entry, innovation incentives, dynamic market structure) that the model does not address.

Table 3 reports the quantitative implication. Evaluating ΔGini at the calibrated values while varying asset concentration and rent-sharing by industry type yields a clear gradient: tech/AI platforms ($\text{Gini}(K) = 0.95$, $\xi = 0.25$) show $\Delta\text{Gini} = +0.022$, while education/government ($\text{Gini}(K) = 0.40$, $\xi = 0.07$) shows $\Delta\text{Gini} = -0.026$. A Scandinavian-style economy with lower concentration but stronger rent-sharing ($\text{Gini}(K) = 0.60$, $\xi = 0.25$) falls

in the equalizing regime ($\Delta\text{Gini} = -0.010$). These cross-industry predictions are testable: within-industry wage inequality trends should correlate positively with industry-level asset concentration.

Table 3: Predicted ΔGini by Industry Type

| Industry Type | Gini(K) | ξ | ΔGini |
|------------------------|-------------|-------|---------------------|
| Tech / AI platforms | 0.95 | 0.25 | +0.0218 |
| Finance / Banking | 0.85 | 0.20 | -0.0002 |
| Healthcare | 0.70 | 0.15 | -0.0143 |
| Manufacturing | 0.65 | 0.15 | -0.0163 |
| Retail / Hospitality | 0.50 | 0.10 | -0.0231 |
| Education / Government | 0.40 | 0.07 | -0.0258 |
| U.S. Baseline (MSM) | 0.91 | 0.20 | +0.0050 |
| Scandinavia-like | 0.60 | 0.25 | -0.0104 |

Notes: ΔGini computed at calibrated values for $\hat{\alpha}/(\phi\mu_h)$, $\hat{\eta}_0$, $\hat{\eta}_1$, varying Gini(K) (asset concentration) and ξ (rent-sharing) by industry type. These scenarios assume proprietary AI ($\psi > \eta_0$); if AI commoditizes via open-source ($\psi < \eta_0$), the concentrating channel reverses (Lemma 1). Higher concentration and stronger rent-sharing both increase ΔGini (Proposition 6). Industries below the line show counterfactual predictions.

Leave-one-out moment sensitivity. A concern with the knife-edge result is that it may be mechanically imposed by including ΔGini as a target moment. Dropping the ΔGini target and re-calibrating from the remaining five moments yields $\Delta\text{Gini} = -0.009$ —in the equalizing regime, but close to the boundary and within the bootstrap CI. The five non- ΔGini moments already constrain the model to produce a near-zero aggregate effect; m_6 provides

incremental discipline on the sign. Parameter values shift modestly: $\hat{\alpha}/(\phi\mu_h)$ moves from 0.526 to 0.524, $\hat{\eta}_1$ from 0.323 to 0.318.

The wage compression ratio has a tight CI of [0.73, 0.85]: AI’s within-task equalizing effect is robustly identified regardless of how the aggregate plays out.

Which moments identify which parameters—and which identify the boundary.

Table 4 reports the formal sensitivity decomposition. Panels A–B show that $\hat{\eta}_1$ is primarily identified by m_4 (top-4 revenue, elasticity +0.71), $\alpha/(\phi\mu_h)$ by m_1 (CV reduction), and σ by m_5 (education premium). Panel C reports the boundary diagnostic: the five non- Δ Gini moments (m_1 – m_5) have *near-zero* boundary influence—they identify the rates of both channels, but opposing parameter shifts nearly cancel in Δ Gini. Only m_6 has substantial boundary influence (pass-through ≈ 1.0). Panel D shows that the concentrating-channel parameters dominate: η_1 (elasticity +9.2) and $\text{Gini}(K_0)$ (elasticity +18.7) exert the largest positive pull, while ξ (+7.5) has comparable effect. All elasticities exceed ± 1 because Δ Gini ≈ 0.005 is near zero, confirming the boundary is genuinely knife-edge. Crucially, η_1 (an AI technology-structure parameter) has a larger derivative than ξ —the boundary is not determined by institutions alone.

3.4 Identification of η_1

The concentration elasticity η_1 captures a structural break rather than a time-series average. We cross-validate the MSM value using two independent sources: (i) Babina et al. [2024], where AI-adopting firms’ 12–18% revenue premium maps to $\eta_1 \in [0.174, 0.190]$; and (ii) Autor et al. [2020], where the 3–7 pp rise in top-4 concentration in AI-intensive sectors maps

Table 4: Moment–Parameter Sensitivity and Boundary Diagnostic

| <i>Panel A: Sensitivity $\partial\hat{\theta}_j/\partial m_i^{\text{data}}$</i> | | | | | | |
|--|----------------------|----------|-------------------------|----------|---------------|---------------|
| | m1 | m2 | m3 | m4 | m5 | m6 |
| $\alpha/(\phi\mu_h)$ | +1.575 | +0.681 | +0.000 | +0.000 | -0.000 | -0.000 |
| σ | +10.854 | +4.691 | -0.000 | +0.000 | -149.991 | -0.000 |
| η_0 | -0.080 | -0.035 | -0.221 | +0.225 | +0.000 | -3.779 |
| η_1 | -0.034 | -0.015 | +0.050 | +0.510 | +0.000 | -1.595 |
| Gini(K_0) | +0.182 | +0.079 | -0.268 | -0.510 | -0.000 | +8.574 |
| <i>Panel B: Elasticity $(\partial\hat{\theta}_j/\partial m_i) \cdot (m_i/\hat{\theta}_j)$</i> | | | | | | |
| | m1 | m2 | m3 | m4 | m5 | m6 |
| $\alpha/(\phi\mu_h)$ | +1.032 | +0.664 | +0.000 | +0.000 | -0.000 | -0.000 |
| σ | +3.209 | +2.063 | -0.000 | +0.000 | -3.217 | -0.000 |
| η_0 | -0.195 | -0.125 | -0.465 | +0.711 | +0.000 | -0.133 |
| η_1 | -0.036 | -0.023 | +0.046 | +0.711 | +0.000 | -0.025 |
| Gini(K_0) | +0.069 | +0.044 | -0.088 | -0.252 | -0.000 | +0.047 |
| <i>Panel C: Boundary Diagnostic—$\Delta(\Delta\text{Gini})$ per +1 SE of moment m_i</i> | | | | | | |
| | m1 | m2 | m3 | m4 | m5 | m6 |
| $\Delta(\Delta\text{Gini})$ | -0.0000 | -0.0000 | -0.0000 | +0.0000 | -0.0000 | +0.0150 |
| As % of ΔGini | -0% | -0% | -0% | +0% | -0% | +300% |
| <i>Panel D: Direct Boundary Sensitivities $\partial(\Delta\text{Gini})/\partial\theta_j$ and $\partial(\Delta\text{Gini})/\partial\xi$</i> | | | | | | |
| | $\alpha/(\phi\mu_h)$ | σ | η_0 | η_1 | Gini(K_0) | ξ [fixed] |
| $\partial(\Delta\text{Gini})/\partial\cdot$ | -0.0135 | +0.0000 | -0.0922 | +0.1430 | +0.1026 | +0.1863 |
| Elasticity | -1.4 | +0.0 | -2.6 | +9.2 | +18.7 | +7.5 |
| <i>Panel E: Primary Identifying Moment (largest elasticity)</i> | | | | | | |
| $\alpha/(\phi\mu_h)$ | m1 (elast. +1.032) | | then m2 (elast. +0.664) | | | |
| σ | m5 (elast. -3.217) | | then m1 (elast. +3.209) | | | |
| η_0 | m4 (elast. +0.711) | | then m3 (elast. -0.465) | | | |
| η_1 | m4 (elast. +0.711) | | then m3 (elast. +0.046) | | | |
| Gini(K_0) | m4 (elast. -0.252) | | then m3 (elast. -0.088) | | | |

Notes: Panels A–B report the sensitivity matrix $S = (G'WG)^{-1}G'W$ and its elasticity transformation. Panel C reports the boundary diagnostic: the chain derivative $\partial(\Delta\text{Gini})/\partial m_i = \sum_j [\partial(\Delta\text{Gini})/\partial\theta_j] \cdot S_{ji}$, evaluated at the calibrated point values and scaled by each moment’s standard error. The five non- ΔGini moments (m_1 – m_5) have near-zero boundary influence: they identify the rates of each channel, but the opposing parameter shifts nearly cancel in ΔGini . Only m_6 (the ΔGini target) has substantial pass-through (≈ 1.0). Panel D reports the direct sensitivities and elasticities of ΔGini with respect to each structural parameter and the fixed rent-sharing elasticity ξ . The concentrating-channel parameters η_1 and Gini(K_0) have the largest positive derivatives; η_0 has a large negative derivative (higher pre-AI elasticity raises the baseline, reducing the gap). The high elasticities reflect proximity to the regime boundary ($\Delta\text{Gini} \approx 0$). Panel E identifies the primary and secondary identifying moment for each parameter.

to $\eta_1 \in [0.315, 0.331]$. The union $[0.174, 0.331]$ contains the MSM point value of 0.323. The discrepancy likely reflects differences in firm populations (technology frontier vs. broader industry). Full details in Online Appendix H.

3.5 Sensitivity Analysis

Figure 2 maps the knife-edge boundary in the parameter space that determines the distributional outcome.

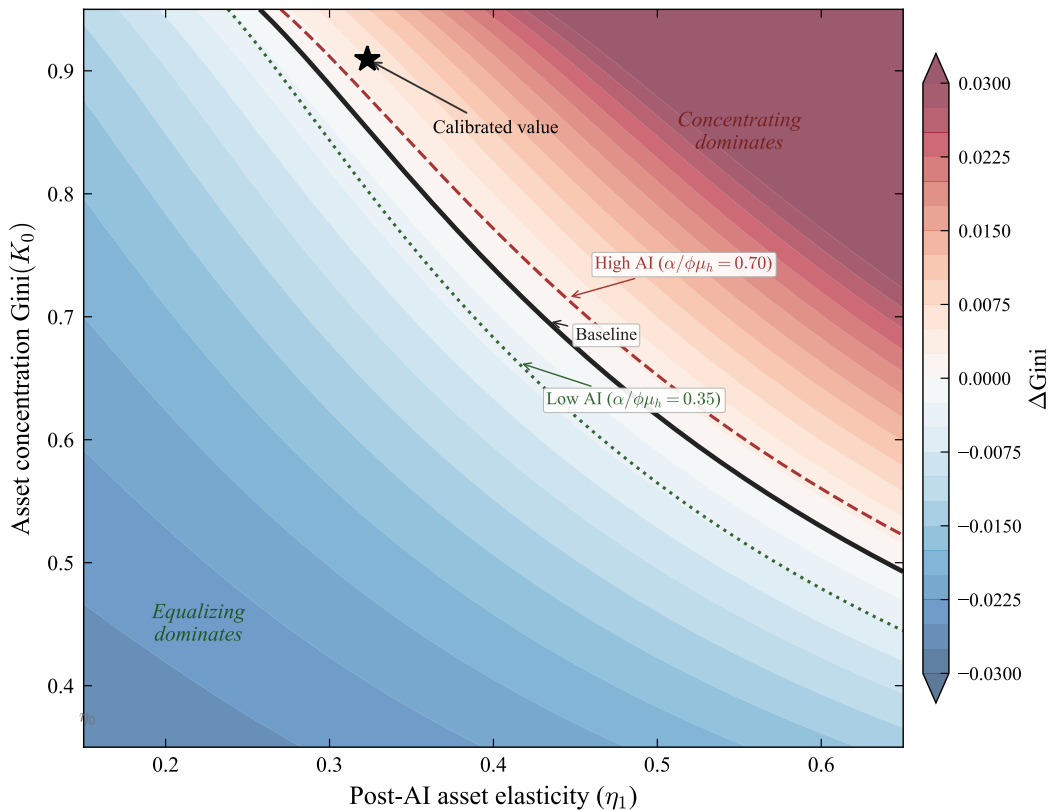


Figure 2: Net inequality effect in $(\eta_1, \text{Gini}(K_0))$ space. Blue: equalizing channel dominates. Red: concentrating channel dominates. Solid black: knife-edge boundary at baseline. Dashed/dotted: boundaries under high/low AI scenarios. Star: calibrated value.

Three features of the contour plot merit comment. First, the knife-edge boundary is nearly linear in this parameter space. Second, the calibrated value sits close to the bound-

ary. Third, stronger AI shifts the boundary: it amplifies both channels, but the knife-edge persists. At any given AI level, the distributional outcome is governed by $(\eta_1, \text{Gini}(K_0))$; but η_1 is itself shaped by AI's technology structure (ψ vs. η_0 , Lemma 1).

Closed-form knife-edge condition. The boundary can be characterized analytically. Under the lognormal approximation for wage variance, AI increases aggregate inequality ($\Delta\text{Gini} > 0$) if and only if the concentrating channel exceeds the equalizing channel:

$$(12) \quad \xi^2 \text{Var}(\log K) \left[\left(\frac{\eta_1}{1 - \gamma_L} \right)^2 - \left(\frac{\eta_0}{1 - \gamma_L} \right)^2 \right] > CV_h^2 \cdot |\mathcal{S}| \cdot \left(1 - \frac{1}{(1 + \alpha/\phi\mu_h)^2} \right).$$

The left-hand side is the increase in between-firm wage variance (through rent-sharing and rising profit elasticity), and the right-hand side is the decrease in within-firm wage variance (through skill homogenization). The condition depends on five measurable quantities: the rent-sharing elasticity ξ , the asset concentration $\text{Var}(\log K)$, the asset elasticity change $\eta_1 - \eta_0$, the ability dispersion CV_h , and the AI output ratio $\alpha/(\phi\mu_h)$. The contour plot visualizes this condition in $(\eta_1, \text{Gini}(K_0))$ space.

What the figure does not show. The exercise assumes static market structure; a dynamic analysis is beyond this paper's scope.

Rent-sharing sensitivity. A key fixed parameter is $\xi = 0.20$. Varying ξ over the empirical range $[0.07, 0.25]$ from Card et al. [2013] reveals that the concentrating channel operates through ξ^2 . At $\xi = 0.07$ (weak rent-sharing), the equalizing channel dominates; at $\xi = 0.25$, the concentrating channel dominates. But ξ and $\text{Gini}(K)$ may co-move: Scan-

dinavian economies with stronger rent-sharing also tend to have lower asset concentration, placing them in the equalizing regime (Table 3). The net effect depends on the cross-country covariance of ξ and $\text{Gini}(K)$.

Table 5: Sensitivity of ΔGini to Rent-Sharing Parameter ξ

| ξ | ΔGini | Regime |
|-------|---------------------|--------------------------|
| 0.00 | -0.0143 | Equalizing |
| 0.05 | -0.0131 | Equalizing |
| 0.07 | -0.0119 | Equalizing |
| 0.10 | -0.0093 | Equalizing |
| 0.15 | -0.0033 | Equalizing |
| 0.18 | +0.0009 | Concentrating (boundary) |
| 0.20 | +0.0050 | Concentrating |
| 0.25 | +0.0153 | Concentrating |
| 0.30 | +0.0280 | Concentrating |

Notes: ΔGini computed at calibrated values for all structural parameters, varying only ξ . Empirical range $\xi \in [0.07, 0.25]$ from Card et al. [2013]. The sign changes near $\xi \approx 0.17$, illustrating that the qualitative effect of AI on inequality is governed by institutional parameters. The rent-sharing parameter enters quadratically (ξ^2) through between-firm wage dispersion. These results assume proprietary AI ($\psi > \eta_0$); if AI becomes commodity ($\psi < \eta_0$), the concentrating channel reverses regardless of ξ (Lemma 1).

AI technology structure sensitivity. Varying the post-AI asset elasticity η_1 while holding $\xi = 0.20$ fixed (Online Appendix H): when $\eta_1 < \eta_0 = 0.142$ (commodity AI, $\psi < \eta_0$), ΔGini is unambiguously negative (-0.019 to -0.014). Even with proprietary AI ($\eta_1 > \eta_0$),

the sign does not flip until $\eta_1 \approx 0.29$. AI’s technology structure is an independent lever: at fixed institutional parameters, varying η_1 alone crosses the regime boundary.

Institution-contingency and AI technology structure. A legitimate objection is that the ξ sensitivity reduces the paper’s AI-specific content to a claim about labor market institutions. The ξ and η_1 sensitivity analyses jointly refute this: varying ξ alone flips the sign, but so does varying η_1 alone. Both are independent levers. AI’s technology structure enters independently through $\psi > \eta_0$ (Lemma 1): whether AI is proprietary ($\psi > \eta_0$, concentrating) or commodity ($\psi < \eta_0$, equalizing) determines $\text{sgn}(\eta'(A))$. The boundary depends on the interaction of AI technology structure and labor institutions—neither factor alone determines the sign. Standard rent-sharing models do not predict simultaneous within-occupation compression and between-firm divergence; standard AI models do not predict that the inequality sign depends on market structure. The joint prediction is novel but conditional on parameters requiring empirical validation.

Full numerical results are reported in Online Appendix D.

3.5.1 Robustness of Homogenization to Multiplicative AI

Proposition 2 shows that homogenization survives under the general specification $y_i = h_i\phi(1 + \beta A) + \alpha A$ provided the additive component dominates. At the calibrated values, homogenization persists for all $\beta < \beta^* \approx 1.10$ —the multiplicative component must exceed the additive component by more than a factor of two before homogenization fails. Even at $\beta = 0.50$ —far beyond any multiplicative effect in existing experiments—the additive channel still dominates ($1.05/0.41 = 2.6\times$ margin). Full numerical results and figures are in Online

4 Evidence and Identification Challenges

We assess the evidence for each link in the mechanism chain, distinguishing what is established, what is suggestive, and what is absent. We close with regressions that illustrate *why naïve tests fail*, motivating the causal designs in Section 5.

Skill compression: strong evidence. Brynjolfsson et al. [2024] ($N = 5,179$ agents), Noy and Zhang [2023] ($N = 444$), and Peng et al. [2023] ($N = 95$) all document compression of the performance distribution, with the largest gains for low-ability workers. The qualifier: Dell’Acqua et al. [2023] find AI hurts performance outside its competence frontier. Homogenization is real within AI’s capability boundary; outside it, AI can widen gaps.

Education returns: suggestive evidence. Direct evidence on AI’s effect on education premia is unavailable. The college premium plateaued for younger cohorts in the 2010s [Autor et al., 2008], and Deming [2017] documents that occupations combining cognitive and social skills experienced faster wage growth—consistent with Proposition 3(c). This link has no direct test yet.

Credential inflation: indirect evidence. Hershbein and Kahn [2018] document technology-driven credential increases in job postings; these findings are consistent with our screening mechanism but were documented for pre-AI shocks. The direct test—whether generative AI exposure drives credential requirements controlling for task content—has not been con-

ducted. This is the weakest link.

Market concentration: strong structural evidence. Industry concentration has risen [Autor et al., 2020], markups have tripled since 1980 [De Loecker et al., 2020], and between-firm wage dispersion accounts for nearly all U.S. earnings inequality growth since 1981 [Song et al., 2019]. Babina et al. [2024] show AI-patenting firms grow faster; Zolas et al. [2024] report AI adoption concentrated in large firms.

Evidence map. Table 6 consolidates the evidentiary status of each mechanism link, the data required for a credible test, and the testable implication that would validate or falsify the link. The table makes transparent that links 2–3 (education returns and credential inflation) have the weakest empirical support and require new data collection efforts.

4.1 The Measurement Mismatch: Why Occupation-Level Data Cannot Test Task-Level Predictions

The model predicts within-task CV compression (Proposition 1), but the natural observable—occupation-level wage dispersion—bundles tasks with heterogeneous ρ plus between-firm rent-sharing and geographic composition. The regressions below are diagnostic, not confirmatory: they document this mismatch.

Using real data from the BLS Occupational Employment and Wage Statistics (OEWS) for May 2019 and May 2023, merged with the AI Occupational Exposure (AIOE) index of Felten et al. [2021] on 6-digit SOC codes (635 detailed occupations matched across years),

Table 6: Evidence Map: Mechanism Links, Existing Evidence, and Required Tests

| Mechanism | Existing Evidence | Evi-Data Needed | Testable Implication |
|--------------------------------------|---|---|--|
| Task homog. (CV ↓) | Brynjolfsson et al. [2024]: raised novice productivity +34% vs. ≈0% for experts; Noy and Zhang [2023]: quality CV ↓ 40% | Within-occupation task-level wages/outputs before & after AI adoption | DiD on within-occupation variance: high-AI exposure tasks should show CV ↓ |
| Education returns shift | Suggestive: Deming [2017] finds social-skill occupations gained faster; college premium plateau | Matched worker education & wages over time; CPS-ASEC × AIOE panel | Education-wage gradient for codifiable skills should decline in high-AIOE occupations ($\sigma > 1$) |
| Credential inflation | Analog: Hershbein and Kahn [2018] find tech shocks raised credential requirements | Longitudinal job posting (Lightcast); level AI adoption | job data firm-creates in required credentials (DiD), controlling for task content |
| Firm concentration (K re-turns ↑) | Babina et al. [2024]: AI firms grow 12–18% faster; Autor et al. [2020]: top-4 share rising | Industry/firm concentration (HHI) over time; sales by AI use | Panel regression: concentration vs. firm AI adoption, controlling for demand shocks |

Notes: Each row corresponds to one link in the mechanism chain (Figure 1). “Existing Evidence” cites the strongest available support. “Data Needed” specifies what a credible causal test requires. “Testable Implication” describes the empirical prediction that would validate or falsify the link. Links 1 and 4 have the strongest support; links 2–3 are model-derived predictions that await direct testing.

we estimate two specifications:

$$(13) \quad \log(p_{90}/p_{10})_o = \beta_0 + \beta_1 \cdot \text{AIOE}_o + \beta_2' X_o + \varepsilon_o,$$

where $\log(p_{90}/p_{10})_o$ is the log ratio of 90th- to 10th-percentile annual wages in occupation o from OEWS, AIOE_o is AI occupational exposure, and X_o includes log median wage. Columns (2) and (5) add 2-digit SOC major occupation group fixed effects to absorb broad skill-level differences across occupation families.

The cross-sectional specification regresses $\log(p_{90}/p_{10})_{o,2023}$ on AIOE and controls (columns 1–2). The first-difference specification regresses $\Delta \log(p_{90}/p_{10})_o$ on AIOE (columns 3–5), removing all time-invariant occupation characteristics.

Table 7: AI Exposure and Within-Occupation Wage Dispersion: Levels vs. First Differences

| | Cross-Section (2023) | | First Difference (2023–2019) | | |
|--|----------------------|-----------|------------------------------|-----------|----------|
| | (1) | (2) | (3) | (4) | (5) |
| AIOE | 0.1088*** | 0.0339** | 0.0167*** | 0.0166*** | 0.0099 |
| | (0.0083) | (0.0161) | (0.0035) | (0.0041) | (0.0083) |
| log(med wage) / Δ log(med wage) | | 0.2445*** | | -0.0074 | -0.0411 |
| | | (0.0327) | | (0.0780) | (0.0788) |
| Design | Levels | Levels | FD | FD | FD |
| Major group FE | No | Yes | No | No | Yes |
| R^2 | 0.208 | 0.520 | 0.034 | 0.034 | 0.163 |
| N | 635 | 635 | 635 | 635 | 635 |

Notes: Columns (1)–(2): dependent variable is $\log(p_{90}/p_{10})$ in 2023 (cross-section). Columns (3)–(5): dependent variable is $\Delta \log(p_{90}/p_{10}) = \log(p_{90}/p_{10})_{2023} - \log(p_{90}/p_{10})_{2019}$ (first difference). Data: BLS OEWS May 2019 and May 2023, merged with the AIOE index (Felten, Raj, and Seamans 2021) on 6-digit SOC codes. Column (2) and (5) include 2-digit SOC major group fixed effects. Robust (HC1) standard errors in parentheses. *** $p < 0.01$, ** $p < 0.05$, * $p < 0.10$. The cross-section (columns 1–2) shows a positive association (composition effect); the first difference (columns 3–5) removes time-invariant occupation characteristics. Neither design identifies a causal effect; see Section 5 for identification strategies.

Table 7 reports the results. In the cross-section (columns 1–2), the coefficient on AIOE is positive and significant: $\hat{\beta}_1 = 0.109$ ($p < 0.01$) unconditionally, declining to 0.034 ($p < 0.05$) with log median wage and major occupation group fixed effects. Occupations with higher AI exposure have *wider* wage dispersion, not narrower—the opposite of Proposition 1’s predic-

tion. Adding 22 major group fixed effects absorbs two-thirds of the positive coefficient (R^2 rises from 0.21 to 0.52), confirming that the positive association largely reflects broad skill-level sorting: high-AIOE occupations are disproportionately cognitive-intensive professional roles with structurally wider pay distributions.

The first-difference specification (columns 3–5) removes all time-invariant occupation characteristics. The bivariate coefficient is +0.017 ($p < 0.01$): occupations with higher AI exposure experienced slightly *larger* increases in dispersion between 2019 and 2023. However, adding major group fixed effects renders the coefficient insignificant (+0.010, $p > 0.10$), with R^2 rising from 0.03 to 0.16. Notably, the mean $\Delta \log(p_{90}/p_{10})$ across all 635 occupations is -0.102 —a 10.2% overall compression of wage dispersion—but this aggregate compression is uncorrelated with AI exposure after controlling for occupation group.

This does not refute the model; it illustrates a fundamental identification problem. The AIOE index measures *exposure potential*—the overlap between an occupation’s task content and current AI capabilities—not *actual AI adoption*. The 2019–2023 period spans only the earliest months of generative AI deployment, far too early for equilibrium wage effects to materialize. The model’s prediction concerns a causal, within-occupation effect of sustained AI deployment—a counterfactual that neither the cross-section nor the short first difference can identify.

Three features of the analysis are instructive. First, cross-section confounds are severe: the composition effect dominates any treatment effect. Second, the 4-year first-difference window is too short relative to AI diffusion timelines. Third, the AIOE measures what AI *could* affect, not what it *has* affected: credible identification requires actual adoption data.

Task composition moderates the AIOE–dispersion relationship: occupations with higher

substitutable-task shares show more compression, consistent with the model, though the effect is not statistically significant given the short window and exposure-vs-adoption gap (Online Appendix I).

What identification design would work. The causal test requires: (i) an occupation \times year panel spanning pre- and post-AI adoption, (ii) firm- or worker-level AI usage intensity replacing static exposure indices, and (iii) within-occupation wage percentile ratios from matched employer-employee data (LEHD, DADS). Staggered DiD estimators [Callaway and Sant’Anna, 2021, Borusyak et al., 2024] would address heterogeneous treatment timing. We leave this to future work.

5 Testable Predictions

The model generates six testable predictions, summarized in Table 8. We sketch identification strategies, informed by the cross-sectional failure documented in Section 4.1: credible tests require time variation in AI adoption, not just cross-sectional exposure indices. H2–H3 (education premium, credential inflation) are conditional on occupations’ task composition—specifically, the mix of substitutable and complementary tasks within each occupation—which the model treats parametrically. These predictions should be tested jointly with task composition data, not extrapolated from the aggregate calibration alone.

The primary identification strategy exploits cross-occupation variation in AI exposure using the AIOE index [Felten et al., 2021] or LLM exposure [Eloundou et al., 2024] in a difference-in-differences framework with staggered adoption estimators [Callaway and Sant’Anna,

Table 8: Testable Predictions

| H | Prediction | Source | Data | Outcome |
|----------|---|---------------|-------------------------|--------------------------------------|
| H1 | Within-occupation output dispersion declines; largest gains for low-ability | Prop. 1 | Task-level productivity | CV, 90–10 gap |
| H2 | Education premium declines in high-AI occupations for codifiable skills (requires $\sigma > 1$; see text) | Prop. 3 | CPS-ASEC × AIOE | Education-wage gradient |
| H3 | Credential requirements rise in high-AI occupations, controlling for tasks (untested prediction; requires post-2023 Lightcast data linked to AI adoption) | Prop. 4 | Lightcast postings | Degree requirement |
| H4 | Between-firm wage dispersion rises; within-firm declines (conditional on $\psi > \eta_0, \xi, \text{Gini}(K)$) | Props. 5, 1 | LEHD matched data | Variance decomposition |
| H5 | AI investment and profits concentrate in high- K firms | Prop. 5(a) | Compustat, ABS | HHI, profit share |
| H6 | Net inequality change depends on AI technology structure (ψ vs. η_0), ξ , and $\text{Gini}(K)$ | Sec. 3 | Cross-industry/country | $\Delta\text{Var}(w)$ vs. HHI, ξ |

2021, Borusyak et al., 2024].

The most direct test of the inequality paradox (H6) would compare inequality decompositions across industries with different concentration levels and AI supply structures: in concentrated industries with proprietary AI ($\psi > \eta_0$), AI should increase between-firm inequality more than it reduces within-firm inequality; in competitive industries or where AI is commoditized ($\psi < \eta_0$), the reverse.

We outline three concrete identification designs, each targeting different links in the mechanism chain.

Design 1: Occupational panel (OEWS/CPS). Construct an occupation \times year panel from BLS OEWS (2015–2028) or CPS-ASEC microdata. Event-study DiD with occupation and year fixed effects, outcome = $\log(p_{90}/p_{10})_{ot}$, treatment = $\text{AIOE}_o \times \mathbf{1}(t \geq 2023)$, using the Callaway and Sant’Anna [2021] estimator. Controls: log median wage, major occupation group trends.

Design 2: Matched firm–worker data. Use LEHD or Census LODS (following Card et al. 2013, Song et al. 2019) with firm-level AI adoption measures. Key outcomes: within-firm wage dispersion $\text{Var}(w_{it}|j)$, between-firm dispersion $\text{Var}(\bar{w}_j)$, and wage elasticity to firm assets. AKM-style decompositions isolate the firm premium ψ_j from worker ability θ_i , directly testing Proposition 5(d).

Design 3: Job postings difference-in-differences. Panel of job ads from Lightcast (2015–2028), using generative AI tool rollouts as treatment. Outcomes: posted wage range (90–10 gap), frequency of degree requirements, and AI-related skill requirements. Instru-

ment: global AI capability shocks (ChatGPT release) interacted with metro-area tech employment shares.

6 Policy Implications

The model identifies three welfare distortions—screening waste from credential inflation, allocative inefficiency from market power, and misallocation of human capital toward AI-replicable skills—and a structural tension between front-loaded displacement costs and gradually accruing productivity gains (Online Appendix E). The model’s contribution to policy thinking is the mechanism, not the verdict: it identifies which levers (ξ , $\text{Gini}(K)$, ψ vs. η_0) determine the sign, without being able to determine the sign itself from the available moments. Within the model, reducing the concentration of AI-complementary assets shifts the economy toward the equalizing regime; promoting open-source AI diffusion (reducing ψ toward or below η_0) weakens the concentrating channel independently of labor market institutions; restricting AI capability impedes the equalizing channel without addressing the concentrating one. Whether these directional implications translate to welfare-improving policy depends on general equilibrium considerations—entry equilibrium, innovation incentives, dynamic market structure—that are beyond this partial-equilibrium model. These are scenario-conditional model implications, not evaluated policy recommendations. Extended welfare analysis is in Online Appendix E.

7 Conclusion

AI compresses task-level skill differences on tasks where human and AI outputs are substitutable. Whether this compression translates into reduced aggregate inequality depends on AI’s technology structure—proprietary ($\psi > \eta_0$, concentrating) vs. commodity ($\psi < \eta_0$, equalizing)—and labor market institutions (ξ , $\text{Gini}(K)$). A scenario analysis via Method of Simulated Moments yields values near the regime boundary. The sensitivity decomposition shows that the five non- ΔGini moments identify the rates of both channels but their effects on the aggregate sign nearly cancel. The sign is pinned by m_6 and ξ at the calibrated parameters; structurally, AI’s technology structure (η_1 vs. η_0) is an independent determinant. The contribution is the mechanism—connecting task-level equalization to firm-level concentration through measurable parameters—not a verdict on which regime the economy inhabits.

We are explicit about what this paper does not establish. It does not identify the aggregate sign, nor does it empirically identify any causal link in the mechanism chain. The occupation-level wage regressions demonstrate a measurement mismatch: the model predicts within-task CV compression, but available data measure occupation-level wage dispersion, which bundles tasks in unknown proportions. Credible tests require within-occupation, within-task data that do not yet exist at scale.

Data and Code Availability

Replication code for the Method of Simulated Moments calibration, bootstrap confidence intervals, sensitivity analyses, and all figures and tables will be posted on a public repos-

itory upon publication. The BLS OEWS wage data (2019–2023) are publicly available from <https://www.bls.gov/oes/>. The AI Occupational Exposure (AIOE) index is available from Felten et al. [2021]. O*NET Work Activities data are available from <https://www.onetonline.org/>. No restricted-access data were used in this paper.

References

Daron Acemoglu. The simple macroeconomics of AI. *NBER Working Paper*, (32487), 2024.

Daron Acemoglu and David Autor. Skills, tasks and technologies: Implications for employment and earnings. In *Handbook of Labor Economics*, volume 4, pages 1043–1171. Elsevier, 2011.

Daron Acemoglu and Pascual Restrepo. The race between man and machine: Implications of technology for growth, factor shares, and employment. *American Economic Review*, 108(6):1488–1542, 2018.

Daron Acemoglu and Pascual Restrepo. Automation and new tasks: How technology displaces and reinstates labor. *Journal of Economic Perspectives*, 33(2):3–30, 2019.

Daron Acemoglu and Pascual Restrepo. Tasks, automation, and the rise in US wage inequality. *Econometrica*, 90(5):1973–2016, 2022.

David Autor, David Dorn, Lawrence F. Katz, Christina Patterson, and John Van Reenen. The fall of the labor share and the rise of superstar firms. *The Quarterly Journal of Economics*, 135(2):645–709, 2020.

- David H. Autor, Frank Levy, and Richard J. Murnane. The skill content of recent technological change: An empirical exploration. *The Quarterly Journal of Economics*, 118(4):1279–1333, 2003.
- David H. Autor, Lawrence F. Katz, and Melissa S. Kearney. Trends in US wage inequality: Revising the revisionists. *The Review of Economics and Statistics*, 90(2):300–323, 2008.
- Tania Babina, Anastassia Fedyk, Alex He, and James Hodson. Artificial intelligence, firm growth, and product innovation. *Journal of Financial Economics*, 151:103745, 2024.
- Simcha Barkai. Declining labor and capital shares. *The Journal of Finance*, 75(5):2421–2463, 2020.
- Gary S. Becker. Investment in human capital: A theoretical analysis. *Journal of Political Economy*, 70(5, Part 2):9–49, 1962.
- Kirill Borusyak, Xavier Jaravel, and Jann Spiess. Revisiting event-study designs: Robust and efficient estimation. *Review of Economic Studies*, 91(6):3253–3285, 2024.
- Erik Brynjolfsson, Danielle Li, and Lindsey R. Raymond. Generative AI at work. *Quarterly Journal of Economics*, 139(3):1721–1784, 2024.
- Brantly Callaway and Pedro H.C. Sant’Anna. Difference-in-differences with multiple time periods. *Journal of Econometrics*, 225(2):200–230, 2021.
- David Card, Jörg Heining, and Patrick Kline. Workplace heterogeneity and the rise of West German wage inequality. *The Quarterly Journal of Economics*, 128(3):967–1015, 2013.

- Jan De Loecker, Jan Eeckhout, and Gabriel Unger. The rise of market power and the macroeconomic implications. *The Quarterly Journal of Economics*, 135(2):561–644, 2020.
- Fabrizio Dell’Acqua, Edward McFowland, Ethan R. Mollick, Hila Lifshitz-Assaf, Katherine Kellogg, Saran Rajendran, Lisa Kraymer, François Candelon, and Karim R. Lakhani. Navigating the jagged technological frontier: Field experimental evidence of the effects of AI on knowledge worker productivity and quality. Working paper, Harvard Business School, 2023.
- David J. Deming. The growing importance of social skills in the labor market. *The Quarterly Journal of Economics*, 132(4):1593–1640, 2017.
- Tyna Eloundou, Sam Manning, Pamela Mishkin, and Daniel Rock. GPTs are GPTs: An early look at the labor market impact potential of large language models. *Science*, 384(6702):ead12347, 2024.
- Maryam Farboodi and Laura Veldkamp. Data and competition. *American Economic Review*, 112(8):2789–2813, 2022.
- Edward W. Felten, Manav Raj, and Robert Seamans. Occupational, industry, and geographic exposure to artificial intelligence: A novel dataset and its potential uses. *Strategic Management Journal*, 42(12):2195–2217, 2021.
- Carl Benedikt Frey and Michael A. Osborne. The future of employment: How susceptible are jobs to computerisation? *Technological Forecasting and Social Change*, 114:254–280, 2017.

- Joseph B. Fuller and Manjari Raman. The emerging degree reset: How the shift to skills-based hiring holds the keys to growing the US workforce at a time of talent shortage. *Harvard Business School Working Paper*, 2022.
- Claudia Goldin and Lawrence F. Katz. *The Race between Education and Technology*. Harvard University Press, Cambridge, MA, 2008.
- Jonathan Haskel and Stian Westlake. *Capitalism Without Capital: The Rise of the Intangible Economy*. Princeton University Press, 2018.
- Brad Hershbein and Lisa B. Kahn. Do recessions accelerate routine-biased technological change? Evidence from vacancy postings. *American Economic Review*, 108(7):1737–1772, 2018.
- Jared Kaplan, Sam McCandlish, Tom Henighan, Tom B. Brown, Benjamin Chess, Rewon Child, Scott Gray, Alec Radford, Jeffrey Wu, and Dario Amodei. Scaling laws for neural language models. *arXiv preprint arXiv:2001.08361*, 2020.
- Jacob Mincer. Schooling, experience, and earnings. 1974.
- Shakked Noy and Whitney Zhang. Experimental evidence on the productivity effects of generative artificial intelligence. *Science*, 381(6654):187–192, 2023.
- Sida Peng, Eirini Kalliamvakou, Peter Cihon, and Mert Demirer. The impact of AI on developer productivity: Evidence from GitHub Copilot. *arXiv preprint arXiv:2302.06590*, 2023.

Jae Song, David J. Price, Fatih Guvenen, Nicholas Bloom, and Till von Wachter. Firming up inequality. *The Quarterly Journal of Economics*, 134(1):1–50, 2019.

Michael Spence. Job market signaling. *The Quarterly Journal of Economics*, 87(3):355–374, 1973.

Nikolas Zolas, Zachary Kroff, Erik Brynjolfsson, Kristina McElheran, David N. Beede, Catherine Buffington, Nathan Goldschlag, Lucia Foster, and Emin Dinlersoz. Advanced technologies adoption and use by US firms: Evidence from the Annual Business Survey. Working paper, NBER, 2024.